Microscopic Simulations of Interlayer Structure and Dynamics in Bihydrated Heteroionic Montmorillonites

V. Marry* and P. Turq

Laboratoire Liquides Ioniques et Interfaces Chargées, case courrier 51, Université P. et M. Curie, 4 Place Jussieu, F-75252 Paris Cedex 05, France

Received: September 17, 2002; In Final Form: December 19, 2002

To simulate the diffusion of a tracer Cs^+ in very compacted bentonites, the interlayer spaces of two bihydrated Na-montmorillonites containing a small quantity of cesium are studied by computer simulations (Monte Carlo and molecular dynamics). The calculated structural properties show that water and sodium cations behave in the same way as in pure homoionic Na-montmorillonites. The study of the dynamical properties shows that simulated self-diffusion coefficients of water are in agreement with short time coefficients measured by neutron scattering. For the ions, the experimental values are related to macroscopic long-time motion and are not directly comparable to simulations. However, the introduction of simulated values in macroscopic models gives results in agreement with tracer experiments.

Introduction

Compacted bentonite clays, mainly composed of sodic montmorillonite, are of great interest for industry and especially for the storage of nuclear waste. They are known for their retention properties toward molecules such as water and ions.

Clays are composed of sheets of aluminosilicate. Montmorillonite is a dioctahedral smectite 2:1—a sheet made up of a layer of octahedral aluminum oxide between two layers of tetrahedral silicon oxides. The ideal formula of a sheet cell is $Si_8Al_4O_{20}(OH)_4$. However, some Al^{3+} and Si^{4+} ions are substituted by cations of a lower valence (Mg^{2+} and Al^{3+}, respectively). That is why clay sheets are negatively charged. Their charge is compensated by counterions, most often Na^+ and Ca^{2+} in natural soils. These sheets are stacked together to form laterally extensive particles, which further aggregate. The spaces between sheets give rise to nanopores called the interlayer porosity, and the interparticle and interaggregate spaces form micro- and macropores. The interlayer porosity is responsible for what is called the "crystalline" swelling of the clay: when a dry clay is brought into contact with water, the sheets draw aside and the counterions located between the sheets are hydrated. Water enters the interlayer space until a monolayer of water is formed. Then, a bi- and a trilayer of water can be formed if the capacity of hydration of the counterion is strong enough to counterbalance the cohesion between sheets. For example, Na-montmorillonites are easily hydrated, but Cs-montmorillonite hydration is stopped at the monolayer state because of the low capacity of hydration of cesium.

When compacted by the application of high pressure, clays constitute a porous homogeneous medium of low permeability. The more compacted the clay, the greater its dry density. Compacting a clay leads to a decrease in pore size. The degree of compactness mainly influences the macroporosity, which is redistributed in meso- and microporosity.[1] Nevertheless, nanoporosity arising from interlayer spacing is not affected. Thus, the proportion of nanoporosity increases with the degree of compactness. It reaches 77% of the total porosity for a dry density of 1.8 kg/L.[2] An evaluation of the pore size leads to 6.6 Å for a bentonite with 50% of swelling clay, compacted to a dry density of 2.0 kg/L.[3] These small pores are well represented by bihydrated interlayer spaces since the diameter of a water molecule is about 3 Å.

Classical models of diffusion in compacted clays are based on the double-layer theory, which is used to describe the system water + cations between two particle surfaces. However, for this pore size, neither the discrete characteristic of water nor the overlap of the electrostatic layers can be neglected. That is why classical models often give results that are far from values obtained from experiments of the diffusion of radionuclides in bentonites compacted above 1.5 kg/L.[3−5]

Microscopic simulations, which give an atomic description of the system, are appropriate tools for modeling clays in low states of hydration. They cannot take into account the geometry of the medium beyond the interlayer region, most often characterized by macroscopic parameters such as porosity, constrictivity, and tortuosity. However, they allow very precise structural and dynamic information on particles in interlayer spaces to be obtained. Until now, microscopic simulations (Monte Carlo and molecular dynamics) have been undertaken in homoionic clays (i.e., those containing only one type of counterion: lithium,[6−9] sodium,[6,7,9−22] potassium,[6,7,9,17,23] cesium,[16,22,24−26] magnesium,[15] calcium[27] or strontium[16]). These simulations have been able to reproduce the discrete swelling properties of the clay, giving structural and dynamical results comparable with experiment. However, a direct comparison of the diffusion coefficients of cations has often been impossible because microscopic models do not take into account the macroscopic geometrical parameters of the clay, which are essential to the interpretation of tracer experiments.[8,19,22,23,26]

In this article, we concentrate on heteroionic clays. To reproduce a situation where a radionuclide such as Cs^+ diffuses into a sodic montmorillonite, we decided to introduce a cesium cation (Cs^+) inside an interlayer space already containing Na^+. Clays are known to segregate; however, it is possible to find,

* Corresponding author. E-mail: marry@ppce.jussieu.fr.

10.1021/jp022084z CCC: $25.00
Published on Web 01/24/2003

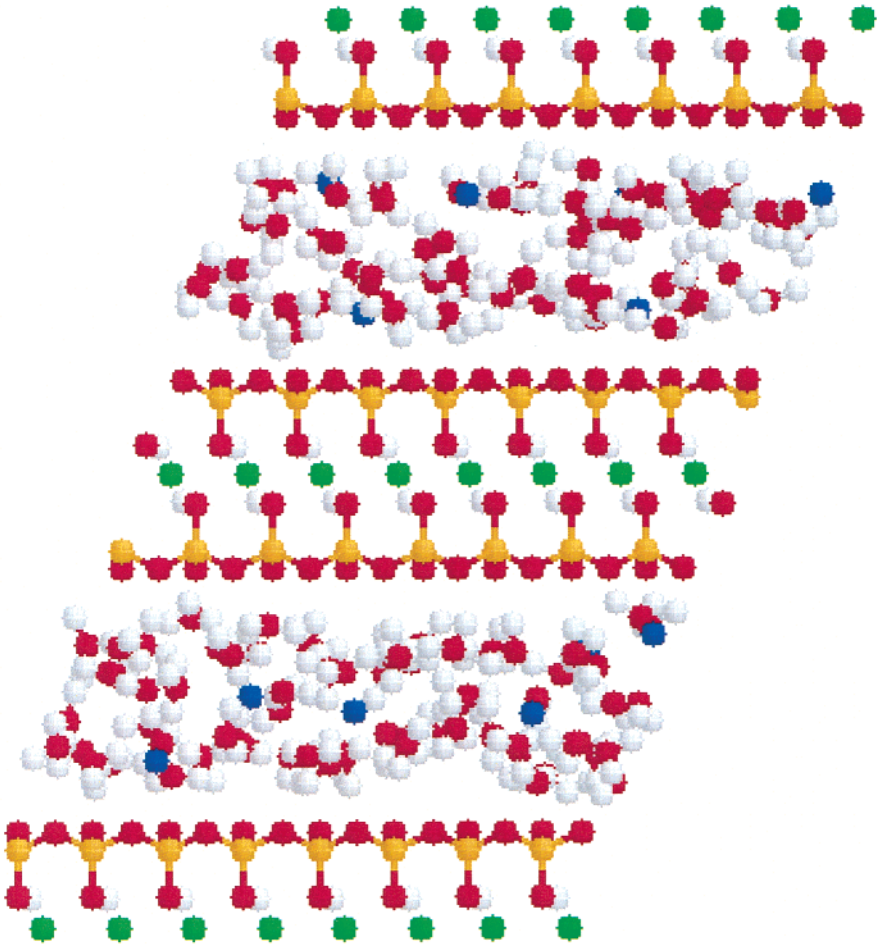

Figure 1. Snapshot of the bihydrated simulation box. Types of atoms: green, Al; yellow, Si; red, O; white, H; blue, counterions.

in particles containing predominantly one type of cation, a trace of another cation.[28,29] Thus, if the pores of a bentonite compacted to 2 kg/L are described by interlayer spaces of 6.6 Å in thickness, it is very probable that diffusing Cs^+ enters these pores in the absence of larger pores. That is why we choose to simulate an interlayer space containing both Na^+ and Cs^+. This new study allowed us to underscore the behavior of water and cations in heteroionic clays. Thus, we were able to calculate diffusion coefficients of cations, which were in agreement with tracer experiments, when introduced into macroscopic models.

Simulation Methods

A. Simulation Box. Two types of montmorillonites were studied: an Otay montmorillonite and a Wyoming montmorillonite. The formulas of their unit cells are $Na_{0.75}[Si_{7.75}Al_{0.25}](Al_{3.5}Mg_{0.5})O_{20}(OH)_4$ and $Na_{0.75}Si_8(Al_{3.25}Mg_{0.75})O_{20}(OH)_4$, respectively. Here, they are called clay 1 and clay 2, respectively. The first clay (clay 1) has been studied extensively.[6,8,10,12,14,15,19,20,23−25] It contains tetrahedral and octahedral substitutions: 0.25 Si^{4+} and 0.5 Al^{3+} are replaced by 0.25 Al^{3+} and 0.5 Mg^{2+}, respectively. The negative charge is thus 0.75e and is counterbalanced by 0.75 Na^+. The second clay contains only octahedral substitutions,[9,14,16,26] also compensated by 0.75 Na^+.

The study of these two clays allows us to enhance the behavioral particularities due to the presence of tetrahedral substitutions. The atomic structure of these montmorillonites was taken from X-ray diffraction measurements.[30,31]

The simulation box is made up of two sheets, each containing eight unit cells. Their dimensions are 20.72 × 17.94 Å^2. Their thickness is 6.54 Å. The sheets are considered to be rigid molecules. They are parallel, and the distance between the centers of two adjacent sheets defines the interlayer spacing.

Each interlayer space contains six counterions. To simulate the introduction of a radionuclide inside a sodic montmorillonite, as explained in the Introduction, the system was first equilibrated with Na^+ cations as counterions to get the characteristics of the pure Na-montmorillonite. Then, a Na^+ per interlayer space was replaced by a Cs^+. Each interlayer space then contained five Na^+ and one Cs^+. The cesium concentration thus obtained is too high since the aim is to describe the diffusion of a tracer element. Nevertheless, it gives an idea of the structural and dynamical behavior of cesium in small quantities in this type of bentonite pores. N water molecules are also introduced into each interlayer space. Figure 1 represents a snapshot of the simulation box with $N = 72$ per interlayer space. The model used for water is the SPC/E model. This model reproduces well the structural and dynamical properties of water. In this model, the molecule is rigid, the O−H distance is 1.0 Å, and the H−O−H angle is 109.47°.

B. Potentials. The interactions between atoms are of the electrostatic and van der Waals type. A Lennard-Jones potential was used for the latter. The potential between two atoms i and j is given by

$$V_{ij} = \frac{q_i q_j}{4\pi\epsilon_0 r_{ij}} + 4\epsilon_{ij}\left[\left(\frac{\sigma_{ij}}{r_{ij}}\right)^{12} - \left(\frac{\sigma_{ij}}{r_{ij}}\right)^{6}\right] \quad (1)$$

where q_i and q_j are the charges of the atoms, r_{ij} is the distance between i and j, and σ_{ij} and ϵ_{ij} are Lennard-Jones parameters

TABLE 1: Charges q and Lennard-Jones Parameters σ_i and ϵ_i of Montmorillonite Atoms and SPC/E Water[a]

	atom	q (e)	σ_i (Å)	ϵ_i (kcal/mol)
clay[24]	Al (o)	3.0	0.0	0.0
	Mg	2.0	0.0	0.0
	Si	1.2	1.84	3.153
	O (a)	−1.0	3.166	0.156
	O (o)	−1.424	3.166	0.156
	O (t)	−0.8	3.166	0.156
	H	0.424	0.0	0.0
water	O	−0.848	3.166	0.156
	H	0.424	0.0	0.0
ion[47]	Na^+	1.0	2.586	0.100
	Cs^+	1.0	3.883	0.100

[a] (o), octahedral; (t), tetrahedral; (a), apical.

given by the Lorentz−Berthelot rules:

$$\sigma_{ij} = \frac{\sigma_i + \sigma_j}{2} \tag{2}$$

$$\epsilon_{ij} = \sqrt{\epsilon_i \epsilon_j} \tag{3}$$

The charges of the clay atoms and their Lennard-Jones parameters are taken from Smith et al.,[24] who were the first to simulate the interlayer spacing of a montmorillonite using the SPC/E model for water. The parameters that are used are summarized in Table 1.

The simulation box consisted of two clay sheets to ensure a vertical half-dimension of the box greater than $2.5 \times 3.166 = 7.915$ Å, where 3.166 Å is the van der Waals radius of water. Then 7.915 Å represents the minimum cutoff distance necessary to calculate interactions between atoms. The long-range electrostatic interactions were treated by means of a 3D Ewald summation.

C. Monte Carlo Simulations. The system clay + water was equilibrated by means of Monte Carlo simulations in the (N, P_z, T) ensemble, where a uniaxial constant pressure normal to the clay sheets was applied. N is the fixed number of water molecules per interlayer space in the simulation box. $P_z = 10^5$ Pa, and $T = 298$ K. N was chosen to correspond to the bilayer state of the interlayer space: $N = 72$.[22]

During these simulations, each molecule is allowed to move with the same probability. The central sheet is restricted to horizontal motion only, but the two-half sheets are allowed to move horizontally and vertically. (See Figure 1.) Depending on the pressure P_z and the degree of hydration N, interlayer spacings will vary until an equilibrium is reached. Sheets are not allowed to rotate. Each molecule is moved randomly. After each motion, the system energy is recalculated, and the new configuration is kept or discarded according to the Metropolis criterion. The system was considered to be equilibrated when the interlayer spacing and the energy oscillated around average values. Further simulations allowed us to obtain structural information such as vertical distributions, correlation functions, and maps of preferential sites along the sheet surface.

D. Molecular Dynamics. Molecular dynamics simulations were performed in the microcanonical (N, V, E) ensemble with the DLPOLY code.[32] Sheets were not allowed to move. Starting configurations were equilibrated configurations obtained previously by Monte Carlo simulations. Trajectories were obtained for simulation times of 320 and 640 ps. The time step was 0.001 ps, and configurations were saved every 40 steps. During these simulations, the energy was kept constant to within about 0.002%.

Self-diffusion coefficients for water molecules and cations Na^+ and Cs^+ were calculated using the 3D Einstein relation

$$D = \lim_{t \to \infty} \frac{\langle \mathbf{r}(t)^2 \rangle}{6t} \tag{4}$$

where $\langle \mathbf{r}(t)^2 \rangle$ is the mean-square displacement of the particle defined by

$$\mathbf{r}(t) = \mathbf{R}(t) - \mathbf{R}(0) \tag{5}$$

where $\mathbf{R}(t)$ is the particle position at time t.

We choose to report values of 3D diffusion coefficients D_{3D} because previous simulations[8,9,23,26] as well as neutron scattering models giving water self-diffusion coefficients have been based on 3D descriptions of the system. However, 2D diffusion coefficients are more appropriate since the vertical motion of particles is limited by the sheet surfaces. Indeed, the mean-square displacements obtained along z were constant as a function of t, giving a null vertical diffusion coefficient for the chosen simulation times. Two-dimensional coefficients are also used in the last part of the article. They are obtained from D_{3D} by multiplication by a factor of $^3/_2$.

Structural Properties

A. Vertical Distributions. After the equilibration of both the sodic montmorillonites clay 1 and clay 2, the equilibrated interlayer spacings were found to be 15.5 and 15.35 Å, respectively, for the bihydrated states ($N = 72$). These results are in the range of experimental data, 15.4−15.5 Å.[33,34] After replacing one Na^+ by one Cs^+ per interlayer space, the systems were reequilibrated in an (N, V, T) ensemble, where the interlayer spacings were fixed at the equilibrated values obtained with Na^+ only. Indeed, we assumed that Cs^+ as a tracer did not influence the global value of the interlayer spacing. Cs^+ was thus immersed into a more confined medium than the pure cesic montmorillonite, whose simulated interlayer spacings are close to 15.6 Å.

Vertical distributions for cations and water molecules in one of the interlayer spaces are presented in Figures 2 and 3 for clay 1 and clay 2, respectively. First, these distributions are very close to those obtained in the corresponding homoionic montmorillonites, even for Cs^+, which is, however, in an environment quite far from that of pure Cs-montmorillonite.[19,22,24] The two peaks of oxygen atom distributions correspond to the location of the two water layers present in the bihydrated states. Cs^+ has the same behavior in both clays, although Na^+ has a tendency to fix to tetrahedral substitutions in clay 1 (the presence of two sharp peaks near the surfaces on Figure 2).[19] Na^+, when not fixed on tetrahedral substitutions, remain in the middle of the interlayer spacing. Indeed, the study of the correlation functions (not shown) shows that the number of water molecules in the first hydration shell of a mobile Na^+ is six, the same as in pure water. On the contrary, Cs^+ has more affinity for the surfaces and approaches them more closely. It has eight water molecules in its first hydration shell, which is lower than its hydration number in pure water (9.2). However, the total solvation number of Cs^+, when the oxygen atoms of water and of the clay surface are taken into account, is equal to its hydration number in pure water. This means that Cs^+ uses the oxygen atoms of the sheet surface to complete its coordination shell.

The presence of two quasi-symmetrical peaks in the cesium distributions shows that the unique Cs^+ of the interlayer space can easily move from one surface to another.

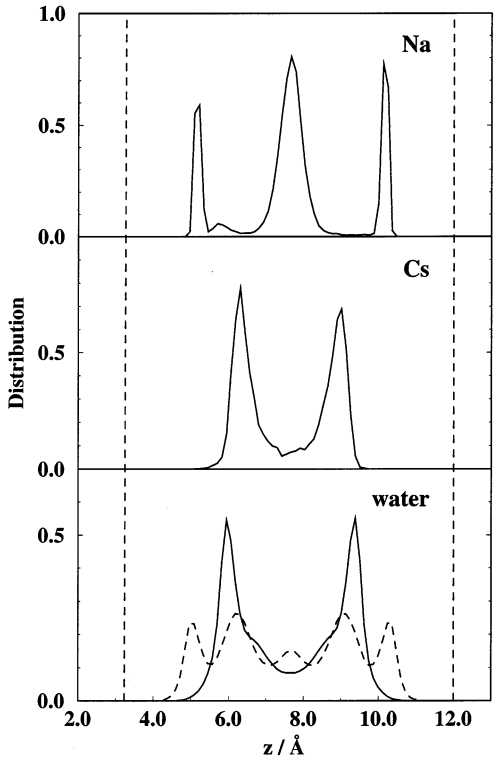

Figure 2. Normalized vertical distributions in an interlayer space of the bihydrated state of heteroionic clay 1. For water: oxygen atoms (—); hydrogen atoms (- -). The vertical dashed lines represent the surface of the clay sheets.

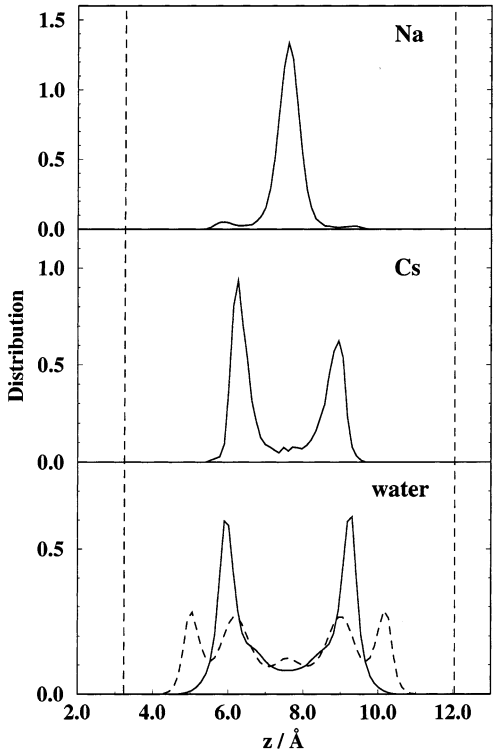

Figure 3. Normalized vertical distributions in an interlayer space of the bihydrated state of heteroionic clay 2. For water: oxygen atoms (—); hydrogen atoms (- -). The vertical dashed lines represent the surface of the clay sheets.

B. Preferential Sites. Viewing Na^+ and Cs^+ trajectories by molecular dynamics allows us to underscore the existence of preferential sites on the surfaces of the sheets. Examples of horizontal (i.e., parallel to the sheets) trajectories for clay 1 are given in Figure 4: the shown Na^+ cations are fixed to tetrahedral substitution sites, as previously seen in simulations on homoionic sodic clays.[19] On the contrary, Cs^+ does not seem to have a preferential attraction to tetrahedral sites. In their article on a homoionic cesic montmorillonite of the clay 1 type, Smith et al.[24] reported that Cs^+ had a tendency to stay close to T sites formed by silicon atoms surrounded by three surface oxygen atoms and to H_t sites formed by the middle of the hexagonal cavities located near tetrahedral substitutions. Here, Cs^+ does not have a particular affinity for H_t sites since tetrahedral substitutions are already compensated by fixed Na^+. However, as in previous simulations,[22,24] Cs^+ is attracted to T sites in the two types of clay, as shown on Figure 5, where only the part of its trajectory that is close to one of the surfaces is represented. No preferential sites or paths were underscored in the case of moving Na^+, probably because their contact with sheet surfaces is not direct but through water molecules.

Maps of preferential sites for constituent atoms of water (O and H, respectively) along surfaces are given in Figures 6 and 7 for clay 2. These maps are more revealing than trajectories. Indeed, to improve the statistics, the horizontal positions of all of the oxygen and hydrogen atoms closer to the surface than a fixed cutoff distance are registered and brought back to the unit cell of the sheet. Figures 6 and 7 represent the sheet surface of the unit cell, with only silicon shown. The cutoff distance is 4.4 Å for oxygen atoms. It corresponds to half the distance between the two surfaces. On vertical distributions shown previously, this means that all of the oxygen atoms contained in the peak near one of the surfaces are taken into account. The cutoff distance for hydrogen atoms is 2.35 Å, which corresponds to the location of the first minimum of the vertical hydrogen distributions: only the hydrogen atoms contained in the small peaks near the surfaces are taken into account. The darker the area, the higher the probability of finding an atom having these dimensions toward the surface of the unit cell.

The maps obtained were similar for both clays. In Figure 6, it is shown that oxygen atoms have a tendency to avoid silicon surface atoms and to move above the hexagonal cavities. In fact, the behavior of an oxygen atom depends partially on the behavior of its corresponding hydrogen atom in direct contact with the surface. The preferential positions of hydrogen atoms in Figure 7 are more pronounced because the atoms that are considered are closer to the surface. Hydrogen atoms avoid silicon atoms but also the middle of the hexagonal cavities. They stay near oxygen surface atoms located between two silicon surface atoms. Thus, they probably form hydrogen bonds with oxygen surface atoms. These bonds would then be very close to the vertical. This is in agreement with previous studies on water molecule orientations in bihydrated Na-montmorillonites.[18,19] Thus, the distance between the first peak of hydrogen distributions and surfaces is about 1.8 Å, which corresponds well to the hydrogen bond length. In view of both maps, these bonds are clearly located in the median planes of covalent Si−O−Si bonds, as in pure water. No preferential interaction has been underscored between water molecules and hydroxyl groups located in the middle of hexagonal cavities, as suggested in some models.[35,36]

Dynamical Properties

Self-diffusion coefficients were determined on linear regions of the mean-square displacement as a function of time. (See Figure 8.) Simulated self-diffusion coefficients of water and cations in both of the bihydrated heteroionic clays are reported in Table 2. In the case of clay 1, the calculated coefficients for

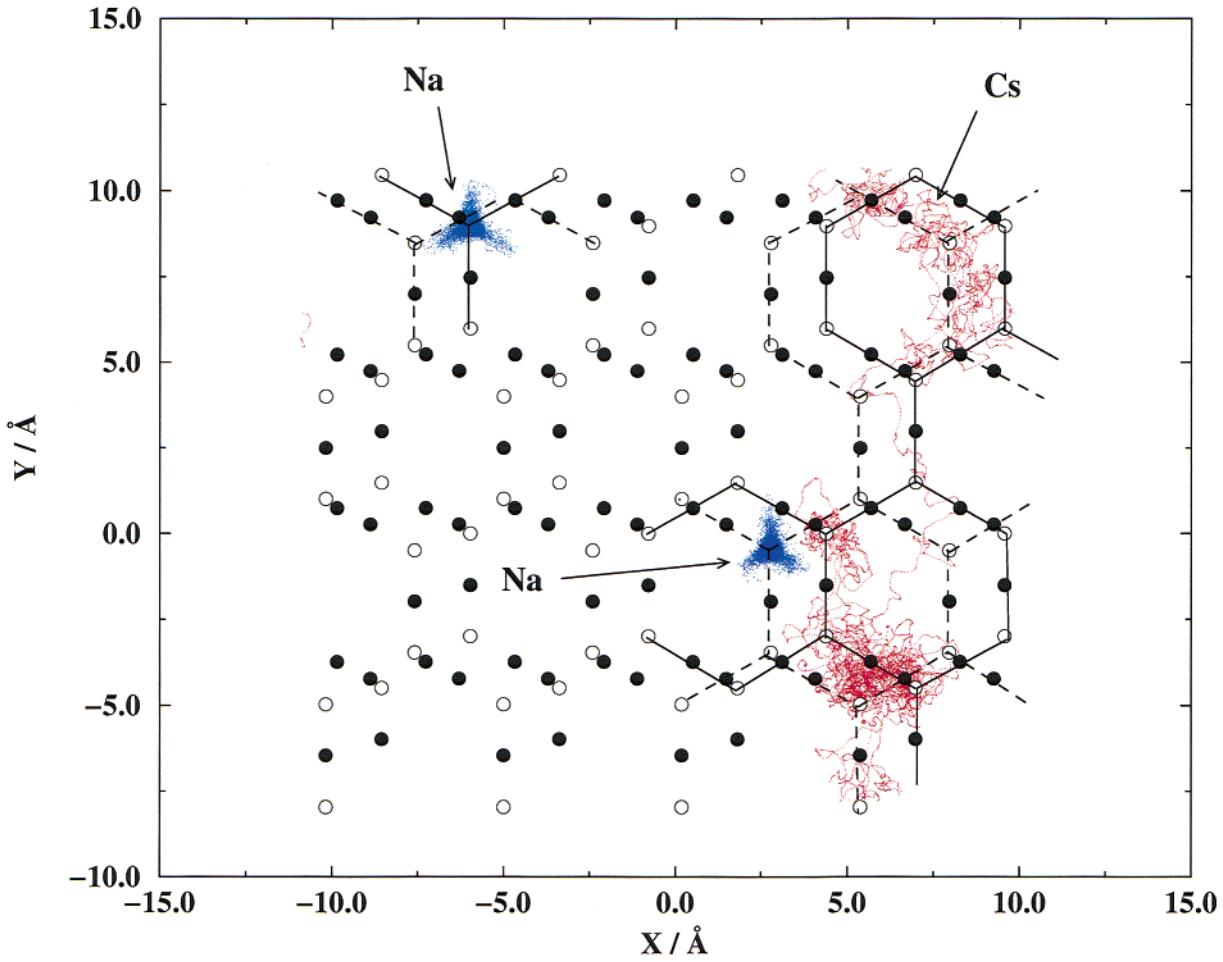

Figure 4. Trajectories of the two fixed Na^+ (blue) and the Cs^+ (red) in one of the interlayer spaces of clay 1. Oxygen surface atoms (●) and silicon surface atoms (○). Solid and dashed lines link silicon atoms of the same surface.

Na^+ include only the mobile cations since Na^+ fixed on tetrahedral substitutions have a null self-diffusion coefficient. As values for diffusion coefficients vary slightly according to the length of the linear region chosen to calculate the coefficients, several values were reported in the Table when the differences were higher than 5%. The values in Table 2 are average values over several simulations with different starting configurations.

According to Table 2, the type of clay does not seem to have an influence on the values of the diffusion coefficients. D_{Cs} is slightly lower in clay 2 than in clay 1, which could be a statistical phenomenon given the small quantity of Cs^+ in the box. However, several simulations were undertaken to improve the statistics. Another explanation could be that in clay 1 the two tetrahedral negative charges are compensated by two fixed Na^+. Then, Cs^+ could be less attracted to the surfaces and more mobile in clay 1 than in clay 2. For hydrated mobile Na^+, which remain in the middle of the interlayer spaces, the charge of the clay could have less influence on the values of the diffusion coefficients. We note that all of the species diffuse about half as fast as in pure water.

To compare these results with those obtained in bihydrated homoionic clays, we undertook simulations with homoionic Na-montmorillonites1 and 2. The self-diffusion coefficients for water were found to be exactly the same as in heteroionic clays. The self-diffusion coefficients for Na^+ were $(6.3-6.8) \times 10^{-10}$ and 5.7×10^{-10} m^2 s^{-1} for homoionic clay 1 and clay 2, respectively. These values are slightly higher than in heteroionic clays, maybe because of the presence of Cs^+, which might perturb the motion of hydrated Na^+. Simulations in homoionic Cs-montmorillonite 2 in the bihydrated state gave a diffusion coefficient for Cs^+ equal to 1.2×10^{-9} m^2 s^{-1}: this is higher than the values in Table 2 probably because here Cs^+ moves in a more confined medium than the corresponding homoionic clay.

The self-diffusion coefficients can be compared with those calculated previously by Chang et al. in bihydrated homoionic Na-montmorillonite of the clay 1 type, with an MCY model for water.[19] Our diffusion coefficients for Na^+ are higher since Chang[8] found 2.5×10^{-10} m^2 s^{-1}. Thus, Chang reports a coefficient equal to 7.9×10^{-10} m^2 s^{-1} for water. These differences probably come from the model used for water. Indeed, the MCY model gives 2.0×10^{-9} m^2 s^{-1} for bulk water,[37] although the coefficient calculated by the SPC/E model[38] is 2.4×10^{-9} m^2 s^{-1}, which is closer to the experimental value:[39] $(2.3-2.4) \times 10^{-9}$ m^2 s^{-1}. The values of the self-diffusion coefficients of water can also be compared with measurements of the diffusion coefficients obtained by neutron scattering. Indeed, this technique allows for the determination of short-time self-diffusion coefficients. Our values are in good agreement with experimental data, which give 1.0×10^{-9} and 8.8×10^{-10} m^2 s^{-1} for sodic homoionic montmorillonite[40] and vermiculite,[41] respectively, and 7×10^{-10} m^2 s^{-1} for Li-montmorillonite.[42]

The comparison of simulated self-diffusion coefficients of cations with experiment is more difficult because most of the experiments on the diffusion of cations are tracer experiments in the steady state and non-steady state.[1,43] These experiments can describe only the long-time behavior of tracers. Steady-

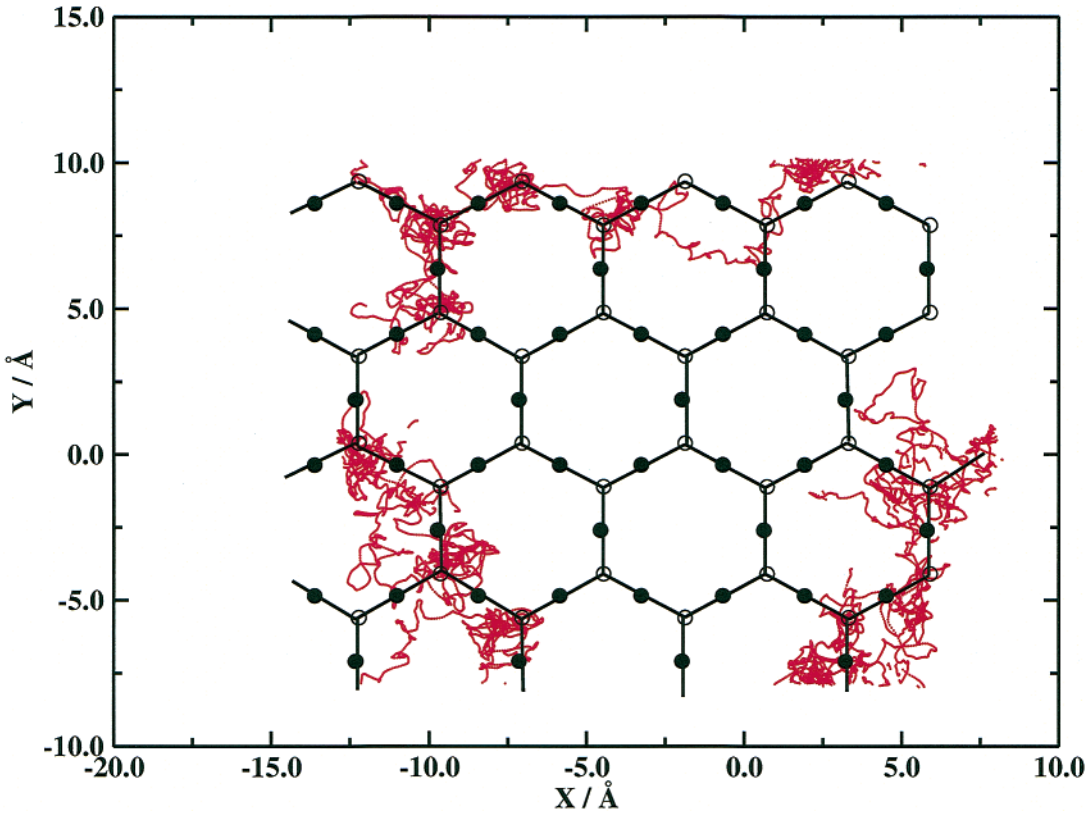

Figure 5. Part of the Cs^+ horizontal trajectory (red line) close to only one of the surfaces, in one of the interlayer spaces of clay 2. Oxygen surface atoms (●) and silicon surface atoms (○).

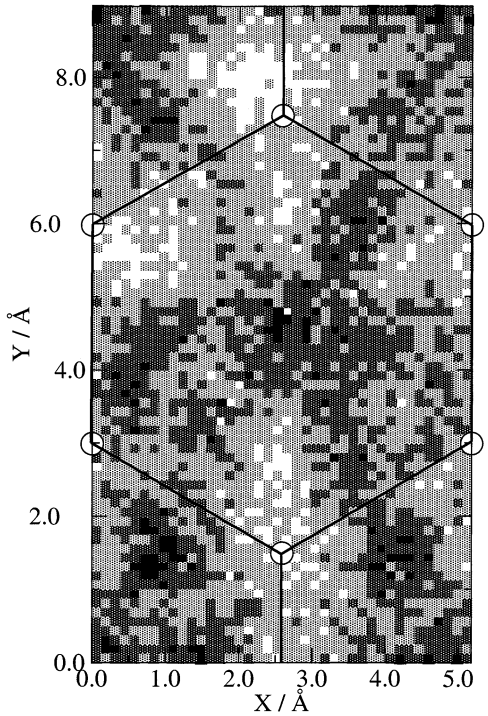

Figure 6. Horizontal map of the preferential sites of water oxygen atoms in bihydrated clay 2. Only atoms less than 4.4 Å from the surface were considered. The darker the area, the higher the probability of finding an oxygen atom with this location toward the surface. Silicon surface atoms are reprensented by gray circles and are linked together by solid lines.

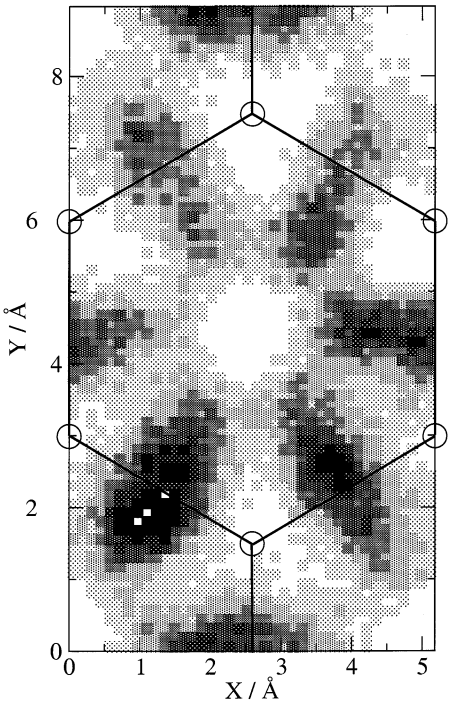

Figure 7. Horizontal map of the preferential sites of hydrogen atoms in bihydrated clay 2. Only atoms less than 2.35 Å from the surface were considered. The darker the area, the higher the probability of finding a hydrogen atom with this location toward the surface. Silicon surface atoms are reprensented by gray circles and are linked together by solid lines.

state experiments allow us to measure the effective diffusion coefficient, which depends on the diffusion coefficient in the pore and on the macroscopic geometry of the system. The non-steady-state experiments lead to the apparent diffusion coefficient, which also depends on fixation reactions in the medium. The values of the apparent diffusion coefficients of Cs^+ are much lower than the simulated ones: they are generally lower

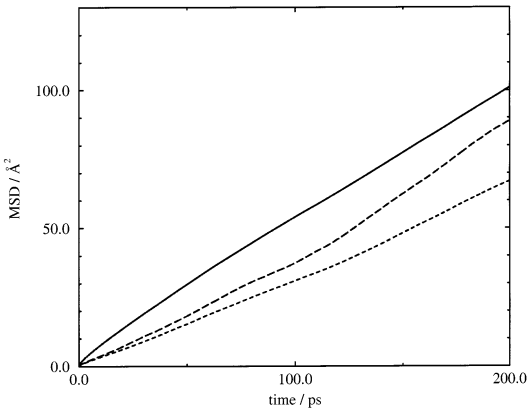

Figure 8. Example of mean-square displacements in clay 2. Only the linear part is shown. The solid line represents the MSD of water molecules. The dashed line represents the MSD of Na^+. The long-dashed line represents the MSD of Cs^+.

TABLE 2: Self-Diffusion Coefficients Obtained by Molecular Dynamics in Heteroionic Clay 1 and Clay 2 in the Bihydrated State[a]

D_{MD} ($m^2\ s^{-1}$)	heteroionic clay 1	heteroionic clay 2
water	1.0×10^{-9}	0.9×10^{-9}
Na^+	$0.53-0.63 \times 10^{-9}$	0.54×10^{-9}
Cs^+	1.0×10^{-9}	0.75×10^{-9}

[a] Coefficients of Na^+ include only the mobile cations.

than 5×10^{-12} $m^2\ s^{-1}$ in clays,[44-46] and Calvet even reported a value of 6×10^{-15} $m^2\ s^{-1}$ for the diffusion of Cs^+ in a clay in a very low state of hydration.[33] However, these long-time values are not comparable with simulated ones since neither chemical reactions nor macroscopic parameters have been taken into account in simulations. To make an accurate comparison, we introduced the simulated values into macroscopic models. Usual models describe the macroscopic geometry of the system through three parameters: the porosity ϵ (the proportion of free volume accessible to the tracer), the constrictivity δ (linked to the section variation of the pore), and the tortuosity τ (expressing the tortuousness of the pore perpendicularly to the global transport of the tracer). The theoretical effective diffusion coefficient is then deduced from the equation

$$D_e = \frac{\epsilon\delta}{\tau^2} D_0 \qquad (6)$$

where D_0 is the diffusion of the tracer in the pore. Most often, macroscopic models describe pores as spaces between two charged planes and use double-layer theories to describe the diffusion inside. However, double-layer theories are not valid when the dry density is higher than 1.5 kg/L, as explained in the Introduction. Nevertheless, simulations allow us to obtain good estimates of D_0 when the clay is in a low state of hydration. Two-dimensional diffusion coefficients must be used in this case. By using the macroscopic parameters given by Kato[3] ($\epsilon = 0.21$, $\delta = 1$, and $\tau \simeq 2.3$) and our simulated value equal to $D_{Cs} = 1.3 \times 10^{-9}$ $m^2\ s^{-1}$ (average of both of the 2D coefficients in clay 1 and clay 2), we found an effective coefficient of 5.2×10^{-11} $m^2\ s^{-1}$. This value corresponds to the effective diffusion coefficient of the tracer Cs^+ in a clay of dry density equal to 2 kg/L. Experimentally, the measurement gives 5×10^{-11} $m^2\ s^{-1}$, although Kato et al. found 3×10^{-10} $m^2\ s^{-1}$ with their macroscopic model. Our value is very close to the experimental one. Thus, an evaluation with the macroscopic parameters reported by Ochs[44,45] ($\epsilon = 0.29$, $\delta = 1$, and $\tau^2 \simeq 9.0$) also gives a good estimate of the effective diffusion coefficient equal to 4.2×10^{-11} $m^2\ s^{-1}$, although Ochs found 4×10^{-10} $m^2\ s^{-1}$ with his model.

The microscopic simulations are then in good agreement with tracer experiments concerning cesium and give better results than the usual macroscopic models in the case of clays in low states of hydration.

Conclusions

To simulate the diffusion of a tracer Cs^+ in a very compacted montmorillonite, we undertook Monte Carlo and molecular dynamics simulations in the bihydrated interlayer space of two different sodic clays, where some Na^+ cations have been replaced by Cs^+ cations. We found that water and Na^+ cations show behavior in the heteroionic clays that is very similar to that in the pure homoionic corresponding clays: if the clay contains tetrahedral substitutions, Na^+ fixes to them. If not, they stay in the middle of the interlayer spaces, surrounded by water molecules.[8,19] On the contrary, Cs^+ has a tendency to remain close to the surfaces, quite near silicon surface atoms. Water, Na^+, and Cs^+ diffuse about half as fast as in pure water. The simulated self-diffusion coefficients of water are in agreement with neutron scattering experiments on bihydrated clays. The simulated self-diffusion coefficients of Cs^+ lead to good evaluations of effective diffusion coefficients, when introduced into macroscopic models. This shows that microscopic simulations are reliable in describing systems under conditions where the double-layer theory is not valid anymore.

Acknowledgment. We thank ANDRA (Agence Nationale pour la Gestion des Déchets Radioactifs) for their financial support.

References and Notes

(1) *Référentiel Matériaux. Tome 2: Les Matériaux Argileux*; Report C.RP.AMAT.1.060/A; ANDRA: Châtenay-Malabry, France, 2001.
(2) Muurinen, A.; Lehikoinen, J. *Evaluation of Phenomena Affecting Diffusion of Cations in Compacted Bentonite*; Nuclear Waste Commission of Finnish Power Companies, Report YJT-95-05, 1995.
(3) Kato, H.; Muroi, M.; Yamada, N.; Ishida, H.; Sato, H. In *Scientific Basis for Nuclear Waste Management*; Murakami, T., Ewing, R. C., Eds.; Materials Research Society: Pittsburgh, PA, 1995; Vol. 18, p 277.
(4) Bourg, I.; Bourg, A.; Sposito, G. *J. Contam. Hydrol.*, in press.
(5) Push, R.; Hömark, H.; Karnland, O. In *Proceedings of the 9th International Clay Conference;* Farmer, V., Tardy, Y., Eds.; Institut de Géologie, Université Louis Pasteur, CNRS: Strasbourg, France, 1990; Vol. 87, p 127.
(6) Boek, E.; Coveney, P.; Skipper, N. *J. Am. Chem. Soc.* **1995**, *117*, 12608.
(7) Park, S.-H.; Sposito, G. *J. Phys. Chem. B* **2000**, *104*, 4642.
(8) Chang, F.-R.; Skipper, N.; Sposito, G. *Langmuir* **1997**, *13*, 2074.
(9) Hensen, E.; Tambach, T.; Bliek, A.; Smit, B. *J. Chem. Phys.* **2001**, *115*, 3322.
(10) Delville, A. *Langmuir* **1992**, *8*, 1796.
(11) Delville, A. *J. Phys. Chem.* **1995**, *99*, 2033.
(12) Boek, E.; Coveney, P.; Skipper, N. *Langmuir* **1995**, *11*, 4629.
(13) Skipper, N.; Sposito, G.; Chang, F.-R. *Clays Clay Miner.* **1995**, *43*, 294.
(14) Skipper, N.; Refson, K.; McConnell, J. *J. Chem. Phys.* **1991**, *94*, 7434.
(15) Skipper, N.; Chang, F.-R.; Sposito, G. *Clays Clay Miner.* **1995**, *43*, 285.
(16) Young, D.; Smith, D. *J. Phys. Chem. B* **2000**, *104*, 9163.
(17) Sposito, G.; Park, S.-H.; Sutton, R. *Clays Clay Miner.* **1999**, *47*, 192.
(18) Delville, A.; Sokolowski, S. *J. Phys. Chem.* **1993**, *97*, 7.
(19) Chang, F.-R.; Skipper, N.; Sposito, G. *Langmuir* **1995**, *11*, 2734.
(20) De Siqueira, A.; Skipper, N.; Coveney, P.; Boek, E. *Mol. Phys.* **1997**, *92*, 1.

(21) Chávez-Páez, M.; Workum, K. V.; de Pablo, L.; de Pablo, J. *J. Chem. Phys.* **2001**, *114*, 1405.
(22) Marry, V.; Turq, P.; Cartailler, T.; Levesque, D. *J. Chem. Phys.* **2002**, *117*, 3454.
(23) Chang, F.-R.; Skipper, N.; Sposito, G. *Langmuir* **1998**, *14*, 1201.
(24) Smith, D. *Langmuir* **1998**, *14*, 5959.
(25) Shroll, R.; Smith, D. *J. Chem. Phys.* **1999**, *111*, 9025.
(26) Sutton, R.; Sposito, G. *J. Colloid Interface Sci.* **2001**, *237*, 174.
(27) Chávez-Páez, M.; de Pablo, L.; de Pablo, J. *J. Chem. Phys.* **2001**, *114*, 10948.
(28) Iwasaki, T.; Watanabe, T. *Clays Clay Miner.* **1988**, *36*, 73.
(29) Glaeser, P.; Méring, J. *Clay Miner. Bull.* **1954**, *2*, 188.
(30) Brindley, G.; Brown, G. *Crystal Structures of Clay Minerals and Their X-ray Identification*; Mineralogical Society, London, 1980.
(31) Maegdefrau, E.; Hofmann, U. *Z. Kristallogr. Kristallgeom. Kristallphys. Kristallchem.* **1937**, *98*, 299.
(32) Smith, W.; Forester, T. CCLRC: Daresbury Laboratory, Daresbury, Warrington, England, 1995.
(33) Calvet, R. *Ann. Agron.* **1973**, *24*, 77.
(34) Fu, M.; Zhang, Z.; Low, P. *Clays Clay Miner.* **1990**, *38*, 485.
(35) Sposito, G.; Prost, R. *Chem. Rev.* **1982**, *82*, 553.
(36) Bérend, I. *Les mécanismes d'hydratation de montmorillonites homioniques pour des pressions relatives inférieures à 0.95*. Thèse de Doctorat, Institut National Polytechnique de Lorraine, Lorraine, France, 1991.
(37) Lie, G.; Clementi, E. *Phys. Rev. A* **1986**, *33*, 2679.
(38) van der Spoel, D.; van Maaren, P.; Berendsen, H. *J. Chem. Phys.* **1998**, *108*, 10220.
(39) Ohtaki, H.; Radnai, T. *Chem. Rev.* **1993**, *93*, 1157.
(40) Hall, P.; Ross, D.; Tuck, J.; Hayes, M. In *Proceedings of the IAEA Symposium Vienna*, Vienna, Austria, 1977; International Atomic Energy Agency: Vienna, Austria, 1978; Vol. 1, p 617.
(41) Swenson, J.; Bergman, R.; Howells, W. *J. Chem. Phys.* **2000**, *113*, 2873.
(42) Cebula, D.; Thomas, R. *Clays Clay Miner.* **1981**, *29*, 241.
(43) Kozaki, T.; Sato, Y.; Nakajima, M.; Kato, H.; Sato, S.; Ohashi, H. *J. Nucl. Mater.* **1999**, *270*, 265.
(44) Ochs, M.; Lothenbach, B.; Wanner, H.; Sato, H.; Yui, M. *J. Contam. Hydrol.* **2001**, *47*, 283.
(45) Ochs, M.; Boonekamp, M.; Wanner, H.; Sato, H.; Yui, M. *Radiochim. Acta* **1998**, *82*, 437.
(46) Eriksen, T.; Jansson, M.; Molera, M. *Eng. Geol.* **1999**, *54*, 231.
(47) Koneshan, S.; Rasaiah, C.; Lynden-Bell, R.; Lee, S. *J. Phys. Chem. B* **1998**, *102*, 4193.